(Received 16 October 2025, Accepted 1 December 2025, Scheduled 23 December 2025)

A Deadbeat Predictive Current Vector Control Algorithm for Improving Current Control Performance of Stepper Motors

Jianmin Ma[1,*] and Kexin Ma[2]

[1] Petroleum Industry Training Center, China University of Petroleum, Qingdao 266580, China
[2] Engineering Training Center, Ocean University of China, Qingdao 266580, China

ABSTRACT: To address the issues of step loss, control lag, and low precision in open-loop hybrid stepper motors applied in economical CNC machine tools, a deadbeat predictive current field oriented control method (DPCFOC) is proposed. First, the research progress of hybrid stepper motor vector control is systematically reviewed, analyzing the advantages and limitations of existing schemes in error compensation, model construction, and algorithm implementation. Subsequently, the continuous mathematical model of the hybrid stepper motor in the rotating coordinate system is established, and the discrete deadbeat predictive model and current prediction equation are derived using the first-order forward Euler method. On this basis, a deadbeat vector control algorithm is proposed. Compared with the traditional dual-closed-loop vector control with PI regulators, the algorithm predicts the next-step current through the motor model and calculates the optimal reference voltage vector in advance to eliminate current error, thereby improving dynamic response speed. Stability analysis via Z-transformation reveals that the system remains stable when the model inductance parameter is within 0–2 times the actual inductance. For the two-phase hybrid stepper motor, a space vector pulse width modulation (SVPWM) strategy based on a dual H-bridge inverter is designed, using 4 non-zero vectors and 2 zero vectors to synthesize the desired voltage vector. Finally, an experimental platform is built with a TMS320F28335 controller and a 57CME22A closed-loop stepper motor to verify the algorithm. This study provides a feasible solution for improving the control precision and dynamic performance of hybrid stepper motors in economical CNC machine tools.

1. INTRODUCTION

In economical CNC machine tools, stepper motors are widely applied in key links such as $X/Y/Z$ axis feed drive, tool magazine rotation, and cooling/lubrication pump flow regulation. Traditional stepper motors mostly adopt subdivision control to achieve open-loop drive; however, the step loss problem under high-speed operation and heavy-load conditions in open-loop mode severely restricts the control accuracy of computer numerical control (CNC) machine tools [1, 2]. Currently, the technology of stepper motors equipped with encoders has become increasingly mature. Applying such motors to economical CNC machine tools can significantly improve the control accuracy of equipment while precisely controlling costs.

Similar to the control logic of permanent magnet synchronous servo motors, vector control schemes for encoder-equipped stepper motors have become a research hotspot in academia, and relevant achievements have been extensively explored. The following content will systematically sort out and analyze the research progress in this field.

In the research field of vector control technology for hybrid stepper motors, scholars have carried out extensive explorations focusing on error compensation, model construction, algorithm implementation, and performance optimization. These efforts have laid a foundation for the development of deadbeat vector control; however, existing studies still have many limitations that need to be addressed.

In terms of achieving low-cost and high-precision control, Reference [3] proposed an error compensation scheme based on a low-cost magnetic encoder. By integrating a linear regression algorithm, it compensates for the first 10 harmonic errors of magnetic resonance position sensor in one go, controlling the position error within 1.2° and achieving a balance between performance and cost. Nevertheless, the scheme's reliance on back electromotive force signals leads to the inability to maintain the extended Kalman filter fusion function when the motor operates at low speeds or is shut down, limiting its applicability across full operating conditions.

In the aspect of motor modeling and control strategy innovation, Ref. [4] constructed an LPV model of the stepper motor in the a-b stationary coordinate system for the first time. It adopted an H_2 optimal gain scheduling strategy, enabling motor operation solely through position feedback and successfully breaking through the bottleneck of speed limitation. However, due to the absence of current sampling and the assumption of an ideal sinusoidal flux linkage, this method is highly sensitive to cogging torque and magnetic saturation, resulting in insufficient robustness under actual operating conditions. Ref. [5] developed a full-process development script from Simulink modeling to board-level verification, which boasts advantages such as strong timing determinism and low PWM jitter. Yet, the idealized motor model it adopted fails to consider cogging effects and saturation characteristics, leading to deviations between simulations and practical applications.

* Corresponding author: Jianmin Ma (mw696@163.com).

For the optimization of control accuracy and dynamic performance, Ref. [6] proposed a backstepping-based torque-current mapping method. By calculating the desired torque τ_d online and converting it into the desired current, it realizes real-time compensation of load and inertia, effectively solving the problem of steady-state lag. Ref. [7] designed a "hybrid modulation" strategy: traditional FOC control with a fixed load angle of 90° is adopted in the high-torque region, while the low-torque region switches to fixed current with adjustable load angle. This strategy addresses the precision defect of commercial high-current drivers under small-current operating conditions. However, since the scheme ignores reluctance and cogging torque, it tends to introduce additional errors during low-speed micro-stepping or sudden load changes. Ref. [8] proposed a control method for online calculation of optimal i_α^* and i_β^*, which avoids reliance on dq transformation and inductance parameters while considering both excitation and reluctance torque. Nevertheless, the method of calculating the command voltage solely through formulas poses the risk of deviation accumulation. Ref. [9] implemented vector control with $i_d = 0$ on a two-phase hybrid stepper motor, combining SVPWM to drive a dual H-bridge structure, which significantly reduces torque ripple and improves system efficiency. However, the experiments were only conducted under low-speed scenarios, and the high-speed performance remains unvalidated.

In terms of algorithm integration and application verification, Ref. [10] applied the FOC algorithm to the stepper motor drive of solar trackers through simulation, effectively enhancing the ability to suppress mechanical backlash and wind disturbance, but lacks hardware experimental support. Ref. [11] verified the adaptability of different high-performance algorithms on stepper motors through multi-algorithm comparison experiments and recommended the PI+SMC combined algorithm for noise-sensitive occasions, providing a reference for the selection of control schemes. Ref. [12] proposed a parallel weighted control structure of power integrity (PI) and sliding mode control (SMC), which dynamically adjusts parameters with a fuzzy algorithm and achieved good results in simulations, but has not yet completed hardware implementation and verification. Ref. [13] modularized the classical FOC, improving its practicability with abundant community cases, yet faces the problem that control performance is difficult to unify and standardize.

Comprehensively, although Ref. [14] systematically sorted out four major control schools — Lyapunov, LPV-H_2, FOC/FWC, and PIpCE — and conducted experimental comparisons, the research only stays at the review level and fails to propose an integrated control framework. Existing studies still have shortcomings in low-cost implementation, full-condition adaptation, model accuracy, parameter robustness, and hardware verification, which provides directions for the further innovation of deadbeat vector control algorithms for hybrid stepper motors.

The above algorithms summarize high-performance control algorithms for stepper motors, but they lack research on how to achieve fast and stable response in stepper motors with encoders. To this end, a DPCFOC method for stepper motors is proposed, achieving high-performance drive control of encoder-equipped stepper motors. Experimental results show that the proposed algorithm has good control effects in terms of current stability and steady-state performance of speed.

2. MATHEMATICAL MODEL OF HYBRID STEPPER MOTOR

2.1. Continuous Model in Rotating Coordinate System

The mathematical model of the hybrid stepper motor in the rotating coordinate system is given as [10]:

$$\begin{cases} u_{\mathrm{d}} = R_{\mathrm{s}} i_{\mathrm{d}} + L_{\mathrm{s}} \frac{\mathrm{d}i_{\mathrm{d}}}{\mathrm{d}t} - \omega_{\mathrm{e}} L_{\mathrm{s}} i_{\mathrm{q}} \\ u_{\mathrm{q}} = R_{\mathrm{s}} i_{\mathrm{q}} + L_{\mathrm{s}} \frac{\mathrm{d}i_{\mathrm{q}}}{\mathrm{d}t} + \omega_{\mathrm{e}} \lambda_{\mathrm{f}} \end{cases} \tag{1}$$

where u_{d} and u_{q} are the d-axis and q-axis voltages respectively; i_{d} and i_{q} are the d-axis and q-axis currents, respectively; R_{s} denotes the stator resistance; L_{s} represents the stator inductance; ω_{e} is the electrical angular velocity of the motor; and λ_{f} stands for the permanent magnet flux linkage.

2.2. Discrete Deadbeat Predictive Model

The first-order forward Euler method is adopted for discretization, and the discrete deadbeat predictive model is expressed as:

$$\begin{cases} u_{\mathrm{d}}(k) = R_{\mathrm{s}} i_{\mathrm{d}}(k) - \omega_{\mathrm{e}} L_{\mathrm{s}} i_{\mathrm{q}}(k) + \frac{L_{\mathrm{s}}}{T_{\mathrm{s}}} \Delta i_{\mathrm{d}}(k) \\ u_{\mathrm{q}}(k) = R_{\mathrm{s}} i_{\mathrm{q}}(k) + \omega_{\mathrm{e}} L_{\mathrm{s}} i_{\mathrm{d}}(k) + \frac{L_{\mathrm{s}}}{T_{\mathrm{s}}} \Delta i_{\mathrm{q}}(k) + \omega_{\mathrm{e}} \lambda_{\mathrm{f}} \end{cases} \tag{2}$$

where k denotes the discrete time step; Δi_{d} and Δi_{q} are the d-axis and q-axis current variations respectively; and T_{s} is the sampling period.

2.3. Current Prediction Equation

The controller samples the actual current vector $i(k)$ at time k, and based on the current reference voltage vector $u(k)$ calculated in the previous step, the predicted current vector $i(k+1)$ for the next step can be obtained. The prediction equation is:

$$\begin{cases} i_{\mathrm{d}}(k+1) = \left(1 - \frac{R_{\mathrm{s}} T_{\mathrm{s}}}{L_{\mathrm{s}}}\right) i_{\mathrm{d}}(k) + \omega_{\mathrm{e}} T_{\mathrm{s}} i_{\mathrm{q}}(k) + \frac{T_{\mathrm{s}}}{L_{\mathrm{s}}} u_{\mathrm{d}}(k) \\ i_{\mathrm{q}}(k+1) = -\omega_{\mathrm{e}} T_{\mathrm{s}} i_{\mathrm{d}}(k) + \left(1 - \frac{R_{\mathrm{s}} T_{\mathrm{s}}}{L_{\mathrm{s}}}\right) i_{\mathrm{q}}(k) \\ \qquad\qquad + \frac{T_{\mathrm{s}}}{L_{\mathrm{s}}} \left(u_{\mathrm{q}}(k) - \omega_{\mathrm{e}} \lambda_{\mathrm{f}}\right) \end{cases} \tag{3}$$

3. DEADBEAT VECTOR CONTROL ALGORITHM

3.1. Deadbeat Vector Control Algorithm and Stability Analysis

3.1.1. Limitations of Traditional Dual-Closed-Loop Vector Control

The block diagram of the traditional dual-closed-loop vector control is shown in Fig. 1. The current loop adopts a PI regulator for current adjustment, which uses the difference between the current command value I_{ref} and the actual value I to generate the reference voltage vector, thereby adjusting the current output to track the command value. This adjustment process has a certain lag; if there is a high demand for the response speed of the current loop, it may easily lead to system instability.

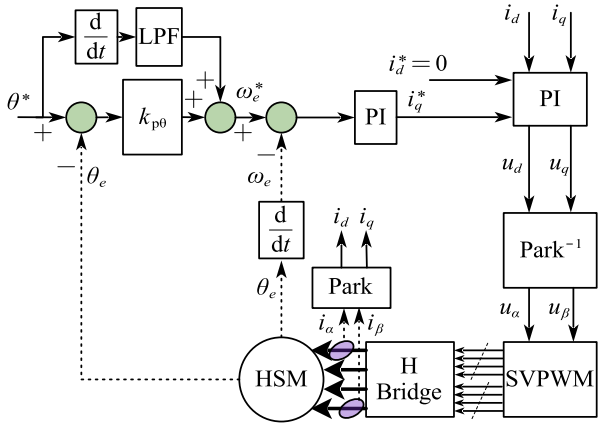

FIGURE 1. Block diagram of traditional dual-closed-loop vector Control.

3.1.2. Principle of Deadbeat Control

The deadbeat method utilizes the mathematical model of the hybrid stepper motor to establish the relationship between the reference voltage vector and current output. It calculates the current prediction value one step in advance and generates the optimal reference voltage vector accordingly [10]. In practical systems, the timing sequence of current loop control is illustrated in Fig. 2.

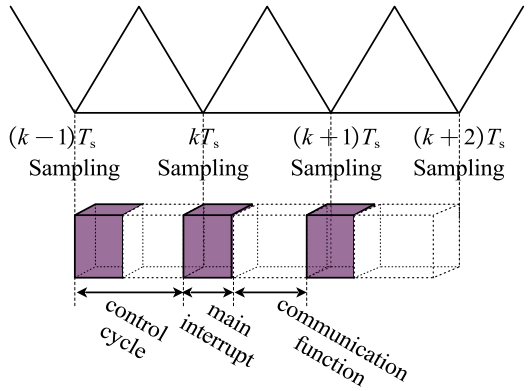

FIGURE 2. Timing diagram of current loop control.

According to Fig. 2, the voltage equation at time k is given by Eq. (2). Since the bandwidth of the speed loop is much smaller than that of the current loop, the influence of speed variation can be neglected within one control cycle. The predicted current for the next step is shown in Eq. (3). Based on the predicted current and reference current, the optimal reference voltage vector $u(k+1)$ that eliminates the current error (i.e., makes the current error zero) can be calculated as:

$$\begin{cases} u_{\mathrm{d}}(k+1) = R_{\mathrm{s}} i_{\mathrm{d}}(k+1) + \omega_{\mathrm{e}} L_{\mathrm{s}} i_{\mathrm{q}}(k+1) + \frac{L_{\mathrm{s}}}{T_{\mathrm{s}}} \Delta i_{\mathrm{d}}(k+1) \\ u_{\mathrm{q}}(k+1) = -\omega_{\mathrm{e}} L_{\mathrm{s}} i_{\mathrm{d}}(k+1) + R_{\mathrm{s}} i_{\mathrm{q}}(k+1) \\ \qquad + \frac{L_{\mathrm{s}}}{T_{\mathrm{s}}} \Delta i_{\mathrm{q}}(k+1) + \omega_{\mathrm{e}} \lambda_{\mathrm{f}} \end{cases} \tag{4}$$

According to the above theory, the control performance of the current loop for hybrid stepper motors can be significantly improved.

3.1.3. Stability Analysis

To analyze the influence of parameter variations on deadbeat control, substituting Eq. (2) into Eq. (3) and calculating with the actual values R_0, L_0, and λ_0 yields:

$$\begin{cases} L_{\mathrm{s}0} i_{\mathrm{d}}(k+1) - L_{\mathrm{s}} i_{\mathrm{d}}^*(k) \\ = (\Delta R_{\mathrm{s}} T_{\mathrm{s}} - \Delta L_{\mathrm{s}}) i_{\mathrm{d}}(k) + \Delta L_{\mathrm{s}} \omega_{\mathrm{e}} T_{\mathrm{s}} i_{\mathrm{q}}(k) \\ L_{\mathrm{s}0} i_{\mathrm{q}}(k+1) - L_{\mathrm{s}} i_{\mathrm{q}}^*(k) \\ = -\Delta L_{\mathrm{s}} \omega_{\mathrm{e}} T_{\mathrm{s}} i_{\mathrm{d}}(k) + (\Delta R_{\mathrm{s}} T_{\mathrm{s}} - \Delta L_{\mathrm{s}}) i_{\mathrm{q}}(k) + \omega_{\mathrm{e}} \Delta \lambda_{\mathrm{f}} T_{\mathrm{s}} \end{cases} \tag{5}$$

where $\Delta R_{\mathrm{s}} = R_{\mathrm{s}} - R_{\mathrm{s}0}$, $\Delta L_{\mathrm{s}} = L_{\mathrm{s}} - L_{\mathrm{s}0}$, and $\Delta \lambda_{\mathrm{f}} = \lambda_{\mathrm{f}} - \lambda_{\mathrm{f}0}$.

Since the sampling time T_{s} is sufficiently small, $\Delta R_{\mathrm{s}} T_{\mathrm{s}}$ can be neglected, and the back electromotive force caused by flux linkage deviation is treated as a disturbance term. Applying the Z-transform to Eq. (5) gives the closed-loop discrete transfer function between the actual current and the reference current:

$$\frac{i_{\mathrm{dq}}^*(z)}{i_{\mathrm{dq}}(z)} = \frac{z - 1 + L_{\mathrm{s}}/L_{\mathrm{s}0}}{(L_{\mathrm{s}}/L_{\mathrm{s}0}) z} \tag{6}$$

From Eq. (6), the closed-loop pole of the discrete transfer function is $z = 1 - L_{\mathrm{s}}/L_{\mathrm{s}0}$. According to control theory, the system is stable when the closed-loop pole lies within the unit circle of the z-plane. Therefore, the stability region of the system is:

$$0 < L_{\mathrm{s}} < 2L_{\mathrm{s}0} \tag{7}$$

It can be seen from Eq. (7) that the deadbeat algorithm converges when the model parameter is less than twice the actual parameter; when the model parameter exceeds twice the actual parameter, the deadbeat algorithm no longer converges, and the system becomes unstable.

3.2. HSM Space Vector Algorithm

3.2.1. Inverter Circuit and Switching States

A typical two-phase hybrid stepper motor (HSM) adopts a dual H-bridge inverter circuit, whose principle is illustrated in Fig. 3. The state of a power switch is denoted as 1 when it is turned on and 0 when it is turned off. The complementary on-off mode is employed for the switches: when the upper switch of a certain bridge arm is on (1), the lower switch of the same arm is off (0), and vice versa. Based on this principle, the inverter has a total of 16 switching states, and each state corresponds to one space voltage vector, resulting in 16 space voltage vectors in total.

3.2.2. Voltage Vector Synthesis

To simplify the operation, four non-zero vectors U_8, U_2, U_4, U_1 and two zero vectors U_0, U_{15} are usually used to synthesize any spatial voltage vector within the limited range. As shown in Fig. 4, the complex plane is equally divided into 4 sectors by the four non-zero voltage vectors. In each sector, the desired spatial voltage vector can be synthesized through vector combination.

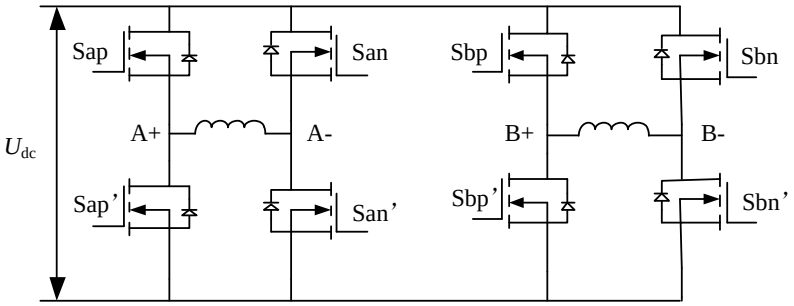

FIGURE 3. Principle of dual H-Bridge inverter circuit.

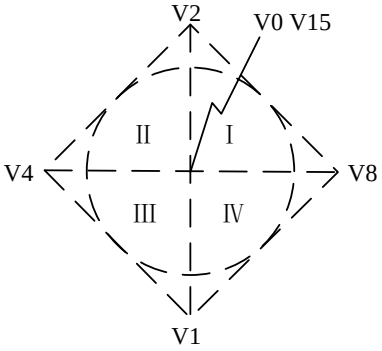

FIGURE 4. Sector division of spatial voltage vectors.

3.2.3. Vector Switching Sequence

Combining Fig. 4 and the vector switching rule table (Table 1), the switching sequence of vectors in each sector can be obtained.

TABLE 1. Correspondence between N value and sector.

Sector	A	B	N
1	0	0	0
2	1	0	1
3	1	1	3
4	0	1	2

To express the relationship between $\boldsymbol{U}_{\text{ref}}$ and sectors conveniently, parameters A and B are defined as follows:

$$A = \begin{cases} 0, & U_\alpha > 0 \\ 1, & U_\alpha \le 0 \end{cases}, \quad B = \begin{cases} 0, & U_\beta > 0 \\ 1, & U_\beta \le 0 \end{cases} \tag{8}$$

A sector-related parameter N is defined as:

$$N = A + 2B \tag{9}$$

The correspondence between the value of N and sectors is shown in Table 2.

TABLE 2. Vector switching sequence.

Sector	Vector Switching Sequence
1	0-8-2-15-2-8-0
2	0-2-4-15-4-2-0
3	0-4-1-15-1-4-0
4	0-1-8-15-8-1-0

This method ensures the accuracy of the spatial voltage at each stage while effectively reducing harmonics and switching losses.

3.3. Proposed Deadbeat Vector Control Algorithm

The block diagram of the proposed deadbeat vector control algorithm for stepper motors is shown in Fig. 5. The implementation process of the SVPWM algorithm is as described in Section 3.2: the sector position is determined by the magnitudes of u_α and u_β input to the SVPWM module, and then the switching

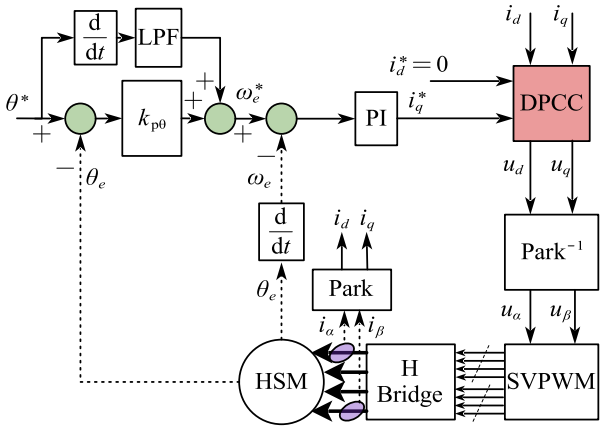

FIGURE 5. Block diagram of the proposed DPCFOC method.

control of power devices is performed according to the vector switching sequence shown in Table 1 [15].

In this control algorithm, a Hall current sensor and a photoelectric encoder are used to sample the current and rotor angle of the HSM (Hybrid Stepper Motor). The sampled i_α and i_β are transformed via the Park transformation to obtain i_d and i_q in the rotating coordinate system. These currents, together with the current command values i_d^* and i_q^*, are input to the DPCFOC for deadbeat control. The entire algorithm relies on the vector control framework, and the dynamic performance of the control system is improved through the deadbeat current control algorithm, laying a foundation for the high-performance application of CNC machine tools.

4. EXPERIMENTAL VERIFICATION

To verify the effectiveness of the proposed algorithm, an experimental platform was built, as shown in Fig. 6. The TMS320F28335 from Texas Instruments was used for algorithm development. The stepper motor used in the test is a 57CME22A closed-loop stepper motor, and the load motor is a permanent magnet synchronous motor.

The specific parameters of the stepper motor used in the test are shown in Table 3.

Figure 7 shows the waveform of the traditional control method under light load (10% rate load) conditions. By observ-

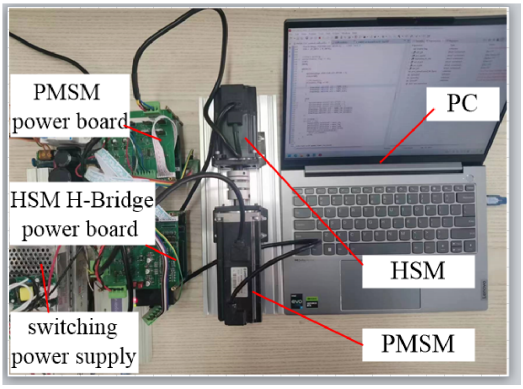

FIGURE 6. Schematic diagram of the experimental platform.

TABLE 3. Parameters of the test stepper motor.

Parameter	Value
Resistance R_s	1.1 Ω
Inductance L_s	5.8 mH
Flux Linkage λ	0.16 Wb
Voltage U	36 V
Current I	4.2 A
Electromagnetic Torque T_e	2.2 N·m
Pole Pairs	50

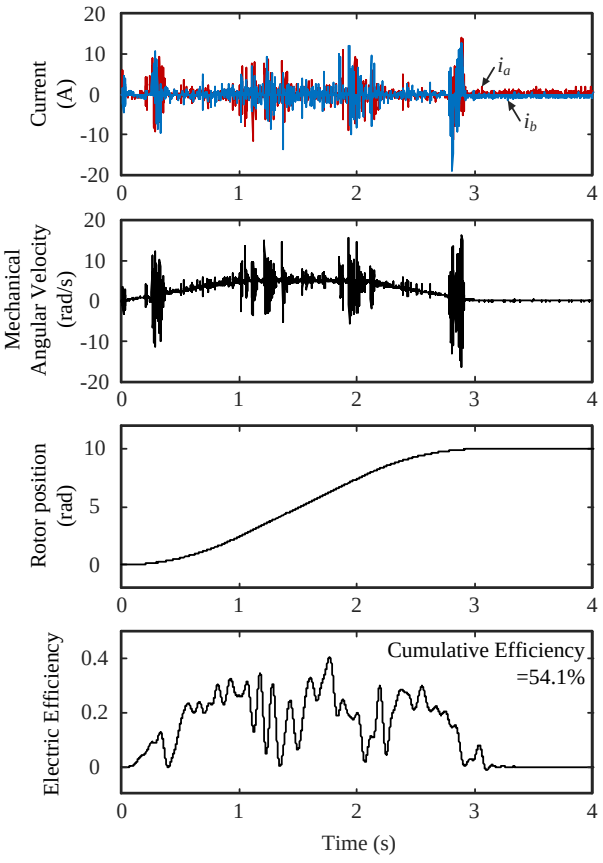

FIGURE 7. The waveform of the traditional control method under light load conditions.

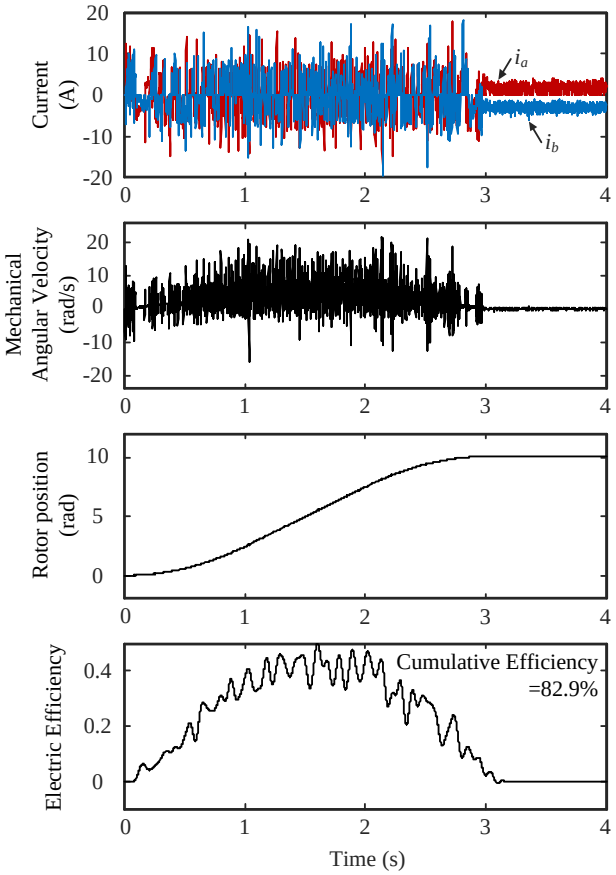

FIGURE 8. The waveform of the traditional control method under heavy load conditions.

ing Fig. 7, it can be found that the traditional control strategy has the following problems: the ia and ib of the motor fluctuate within the range of −10 A to 10 A. Within the time domain of 0–3 s, multiple current mutations occur, with a maximum instantaneous deviation of 15 A. The mechanical angular velocity fluctuates between −20 rad/s and 20 rad/s, and obvious speed spikes appear at 0.5 s, 1.5 s, and 2.5 s. The maximum speed deviation is 12 rad/s, and the speed fluctuation rate is as high as 60%. The fluctuation range of electrical efficiency is large, and the cumulative efficiency is 54.1%. It can be concluded that under light-load conditions, the traditional control suffers from problems such as significant current oscillation, poor speed stability, and large angle error. The lag of its proportional-integral regulation results in insufficient current tracking accuracy, which easily leads to the risk of motor step loss.

Figure 8 shows the waveform of the traditional control method under heavy load (95% rate load) conditions. The current fluctuation of ia and ib of the motor under the traditional control remains within the range of −20 A to 20 A; the fluctuation amplitude does not ease significantly, and the current response delay reaches 0.3 s, which fails to adapt to load changes in a timely manner. The fluctuation amplitude of the angular velocity is still between −20 rad/s and 20 rad/s, accompanied by a continuous speed drop and a maximum speed loss of 10 rad/s, leading to a significant decline in system stability. The

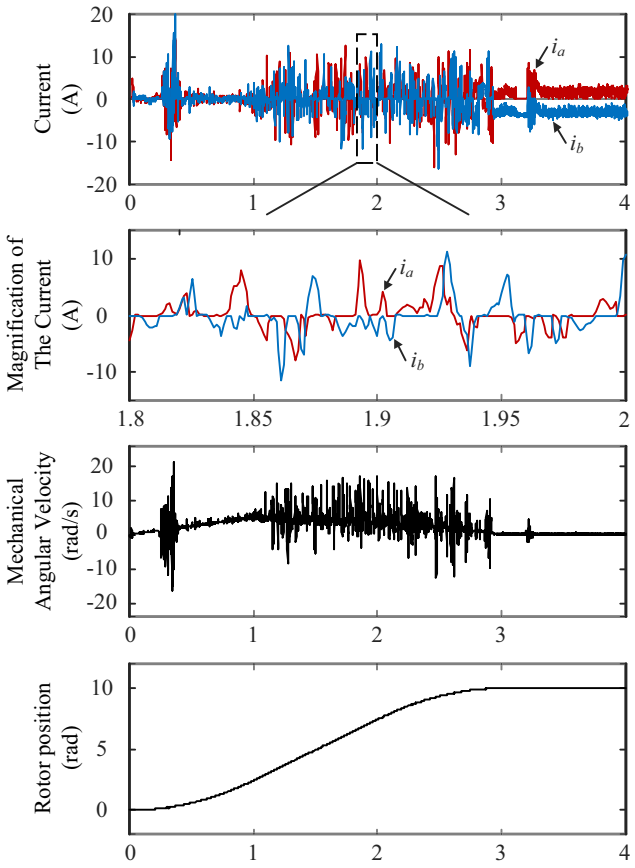

FIGURE 9. The waveform of the traditional control method under variable load conditions.

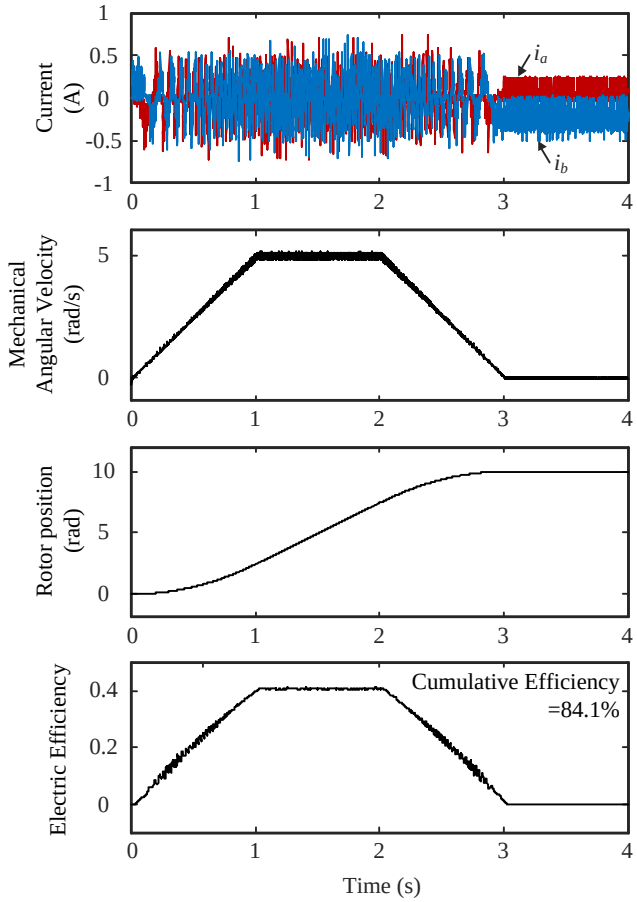

FIGURE 10. The waveform of the proposed DPCFOC method under light load conditions.

fluctuation range of the electrical efficiency is quite large, and the cumulative efficiency is 82.9%. Obviously, under heavy-load conditions, the traditional control has prominent issues, including aggravated current response delay, speed instability, and large angle error; its proportional integral regulator is prone to integral saturation, which cannot meet the requirements of economical CNC machine tools for dynamic performance and control accuracy.

Figure 9 shows the waveform of the traditional control method under variable load conditions. The traditional control strategy exhibits the following issues: the motor phase currents, ia and ib, show pronounced fluctuations; the locally enlarged current waveforms reveal obvious oscillations during load changes, indicating an unstable system response to load variations. The mechanical angular velocity undergoes severe fluctuations when the load varies. Although the rotor position curve increases overall, its rate of change becomes unstable under varying loads. These suggest that the control strategy lacks sufficient robustness and dynamic performance in handling load variations and requires further optimization to enhance system stability and response speed.

Figure 10 shows the waveform of the proposed DPCFOC method under light load (10% rate load) conditions. The proposed DPCFOC method exhibits significantly better performance than the traditional control, with specific characteristics as follows: the phase current fluctuation is effectively suppressed within the range of -0.5 A to 0.5 A; the current ripple coefficient is reduced by 96.7% compared with the traditional control, and there is no obvious current mutation. The speed fluctuation rate is reduced to 20%, and there is no speed spike issue. Meanwhile, the dynamic response speed is 3 times faster than that of the traditional control. The fluctuation of electrical efficiency is stable, and the cumulative efficiency is 84.1%. It can be seen that under light-load conditions, the DPCFOC method effectively eliminates current errors by predicting the current in advance and generating the optimal voltage vector. This further significantly improves the current tracking accuracy, speed stability, and angle control accuracy, and fundamentally avoids the risk of motor step loss.

Figure 11 shows the waveform of the proposed DPCFOC method under heavy load (95% rate load) conditions. The phase current fluctuation is limited within the range of -3.6 A to 3.6 A. The current response delay is shortened to 0.05 s, which is an 83.3% reduction compared with the traditional control, enabling rapid tracking of load changes. The speed stability is improved by 80% relative to the traditional control, with no system instability observed. The fluctuation of electrical efficiency is stable, and the cumulative efficiency is 88.7%. It can be concluded that under heavy-load conditions, the DPCFOC method fundamentally avoids the integral saturation issue that PI regulators are prone to, by virtue of the discrete prediction model and Z-transformation stability design. Meanwhile,

TABLE 4. Comparison table of stepper motor performance data.

Project	FOC	DPCFOC	DPCFOC VS FOC
	Ligh/heavyt-load	Ligh/heavyt-load	Ligh/heavyt-load
Current fluctuation (A)	33.00 / 41.12	5.89 / 9.10	82.2%↓ / 77.9%↓
Speed fluctuation (rad/s)	32.55 / 10.03	10.00 / 10.00	69.3%↓ / 0.3%↓
Cumulative Efficiency	54.1% / 82.9%	84.1% / 88.7%	55.5%↑ / 7%↑

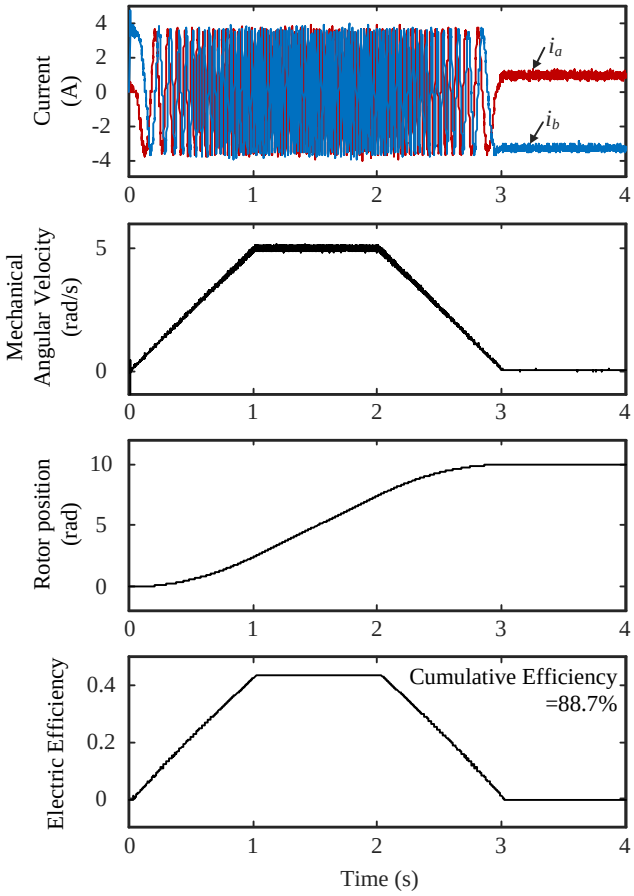

FIGURE 11. The waveform of the proposed DPCFOC method under heavy load conditions.

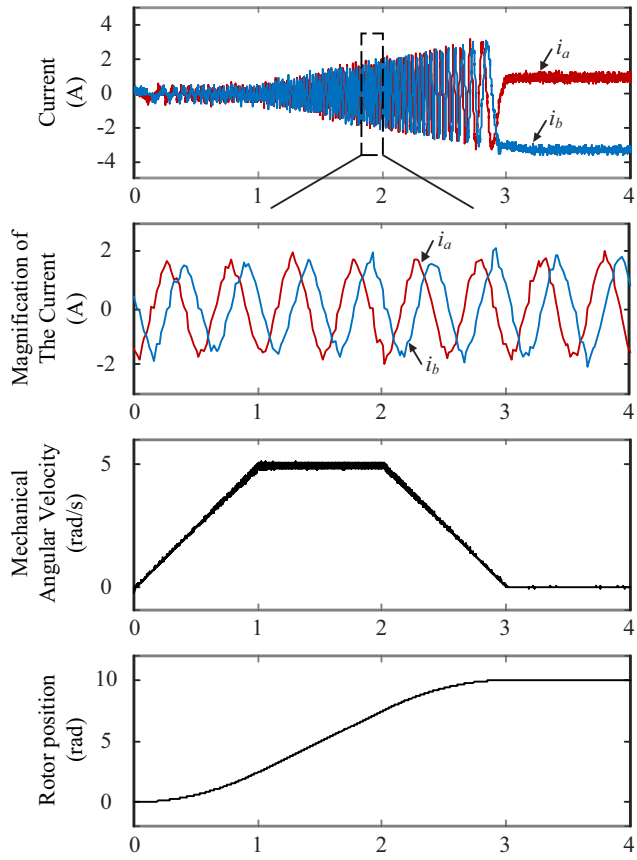

FIGURE 12. The waveform of the proposed DPCFOC method under variable load conditions.

combined with the SVPWM vector synthesis strategy, it can effectively suppress torque ripple, ensure stable system operation, and fully meet the high-precision control requirements of economical CNC machine tools under heavy-load conditions.

Figure 12 shows the waveform of the proposed DPCFOC method under variable load conditions. The proposed DPCFOC method performs significantly better than the traditional control method. Its specific features are as follows: the phase currents, ia and ib, can rapidly stabilize with small fluctuations when the load changes; the locally enlarged current waveforms show ideal sinusoidal shapes, indicating that the method has a superior dynamic response and stability and can effectively suppress current fluctuations. The mechanical angular velocity can quickly return to the set value when the load varies, and the rotor position maintains a relatively smooth change with small deviation, demonstrating that the method achieves better speed control performance and position control accuracy.

Table 4 shows the comparison results of current fluctuation, speed fluctuation, and efficiency ratio. From these data, it can be seen that the proposed algorithm has smaller fluctuations in current and speed, and higher motor efficiency.

5. CONCLUSION

This study proposes a vector control algorithm for stepper motors based on a deadbeat predictive current method. Firstly, by systematically reviewing existing technologies, the limitations of traditional PI dual closed-loop vector control in terms of dynamic response were identified. To address this, a continuous mathematical model of a hybrid stepper motor in a rotating coordinate system was established, and its discretized deadbeat predictive model and current prediction equation were successfully derived. Based on this model, an advanced deadbeat vector control algorithm was proposed. The core of this algorithm lies in using the motor model to predict the next

current and calculating the optimal reference voltage vector in advance, thereby achieving feedforward compensation and elimination of current errors, significantly improving the system's dynamic response speed and control accuracy. Theoretical analysis proves that the algorithm has good robustness, and stability analysis shows that even when there is a certain deviation in the model inductance parameter (within the range of 0 to 2 times the actual inductance), the control system can still maintain stable operation. Additionally, for a two-phase hybrid stepper motor, we designed and implemented a SVPWM strategy based on a dual H-bridge inverter, effectively synthesizing the desired voltage vectors. Finally, the feasibility and superiority of the proposed deadbeat vector control algorithm were fully confirmed through experimental verification on an experimental platform based on a TMS320F28335 controller. In summary, this study not only provides a high-performance closed-loop control solution for hybrid stepper motors but also lays a solid technical foundation for enhancing the overall performance and competitiveness of economical CNC machine tools.

REFERENCES

[1] Liu, X., Y. Pan, Y. Zhu, H. Han, and L. Ji, "Decoupling control of permanent magnet synchronous motor based on parameter identification of fuzzy least square method," *Progress In Electromagnetics Research M*, Vol. 103, 49–60, 2021.

[2] Zhu, L., B. Xu, and H. Zhu, "Interior permanent magnet synchronous motor dead-time compensation combined with extended Kalman and neural network bandpass filter," *Progress In Electromagnetics Research M*, Vol. 98, 193–203, 2020.

[3] Zhou, C. and B. Liu, "A hybrid stepper motor control solution based on a low-cost position sensor," in *2019 IEEE International Conference on Mechatronics and Automation (ICMA)*, 1836–1841, Tianjin, China, 2019.

[4] Lee, Y., D. Shin, W. Kim, and C. C. Chung, "Nonlinear H2 control for a nonlinear system with bounded varying parameters: Application to PM stepper motors," *IEEE/ASME Transactions on Mechatronics*, Vol. 22, No. 3, 1349–1359, 2017.

[5] Lai, C.-K., J.-S. Ciou, and C.-C. Tsai, "FPGA-based stepper motor vector control system design," in *2017 International Automatic Control Conference (CACS)*, 1–5, Pingtung, Taiwan, 2017.

[6] Kim, W., D. Shin, and C. C. Chung, "Microstepping with nonlinear torque modulation for permanent magnet stepper motors," *IEEE Transactions on Control Systems Technology*, Vol. 21, No. 5, 1971–1979, 2013.

[7] Sarr, M. P., M. F. Ndiaye, B. Dieng, and A. Thiam, "Field oriented control of stepper motors for a mini heliostat tracking," in *2021 IEEE 1st International Maghreb Meeting of the Conference on Sciences and Techniques of Automatic Control and Computer Engineering MI-STA*, 104–109, Tripoli, Libya, 2021.

[8] Jeong, Y. W., Y. Lee, and C. C. Chung, "A survey of advanced control methods for permanent magnet stepper motors," *Journal of Marine Science and Technology*, Vol. 28, No. 5, 2, 2020.

[9] Ricci, S. and V. Meacci, "Simple torque control method for hybrid stepper motors implemented in FPGA," *Electronics*, Vol. 7, No. 10, 242, 2018.

[10] Bernardi, F., E. Carfagna, G. Migliazza, G. Buticchi, F. Immovilli, and E. Lorenzani, "Performance analysis of current control strategies for hybrid stepper motors," *IEEE Open Journal of the Industrial Electronics Society*, Vol. 3, 460–472, 2022.

[11] Li, C., S. Tang, M. Yin, X. Zhao, and H. You, "Enhancing position tracking of hybrid stepper motors using lyapunov-based current controllers," *Electronics*, Vol. 14, No. 10, 1997, 2025.

[12] Paul, M. J. and D. Mathew, "A novel vector control strategy for bipolar stepper motor," *International Journal of Scientific & Engineering Research*, Vol. 5, No. 11, 1133–1139, 2014.

[13] Lixian, S. and W. Rahiman, "A compound control for hybrid stepper motor based on PI and sliding mode control," *IEEE Access*, Vol. 12, 163 536–163 550, 2024.

[14] Skuric, A., H. S. Bank, R. Unger, O. Williams, and D. González-Reyes, "SimpleFOC: A field oriented control (FOC) library for controlling brushless direct current (BLDC) and stepper motors," *Journal of Open Source Software*, Vol. 7, No. 74, 4232, 2022.

[15] Rahmatullah, R., A. Ak, and N. F. O. Serteller, "Design of sliding mode control using SVPWM modulation method for speed control of induction motor," *Transportation Research Procedia*, Vol. 70, 226–233, 2023.